Published in final edited form as:
J Biomed Nanotechnol. 2009 April ; 5(2): 151–161.

Development of Idarubicin and Doxorubicin Solid Lipid Nanoparticles to Overcome Pgp–mediated Multiple Drug Resistance in Leukemia

Ping Ma[1], **Xiaowei Dong**[2], **Courtney L. Swadley**[2], **Anshul Gupte**[2], **Markos Leggas**[2], **Harry C. Ledebur**[3], and **Russell J. Mumper**[1,4,*]

[1]Division of Molecular Pharmaceutics, Center for Nanotechnology in Drug Delivery, UNC Eshelman School of Pharmacy, University of North Carolina at Chapel Hill, Chapel Hill, NC 27599, USA

[2]Department of Pharmaceutical Sciences, College of Pharmacy, University of Kentucky, Lexington, KY 40536, USA

[3]NanoMed Pharmaceuticals Inc., Kalamazoo, MI 49009, USA

[4]UNC Lineberger Comprehensive Cancer Center, University of North Carolina at Chapel Hill, NC 27599, USA

Abstract

The objectives of these studies were to investigate and compare solid lipid nanoparticles (SLNs) of two anthracyclines, idarubicin (IDA) and doxorubicin (DOX), against Pgp-mediated multiple drug resistance (MDR.) *in-vitro* and *in-vivo* using different human and murine cancer cell models. IDA and DOX SLNs were developed from warm microemulsion precursors comprising emulsifying wax as the oil phase, and polyoxyl 20-stearyl ether (Brij 78) and D-alpha-tocopheryl polyethylene glycol succinate (Vitamin E TPGS) as the surfactants. Anionic ion-pairing agents, sodium taurodeoxycholate (STDC) and sodium tetradecyl sulfate (STS), were used to neutralize the charges of the cationic anthracyclines and enhance entrapment of the drugs in the SLN. The *in-vitro* cytotoxicity results showed that the IC_{50} value of DOX NPs was 9-fold lower than that of free DOX solution in resistant P388/ADR cell line. In contrast, free IDA had comparable IC_{50} values as IDA NPs in Pgp-overexpressing P388/ADR and HCT-15 cells. In the *in-vivo* P388/ADR leukemia mouse model, the median survival time of DOX NPs was significantly greater than that of free DOX, and controls. In contrast, free IDA was equally as effective as IDA NPs in P388 and Pgp-overexpressing HCT-15 mouse tumor models. The cell uptake of IDA formulated as free IDA and IDA NPs was comparable in Pgp-overexpressing cells. In conclusion, DOX NPs could overcome Pgp-mediated MDR both *in-vitro* in P388/ADR leukemia cells and *in-vivo* in the murine leukemia mouse model. The present study suggests that our SLNs may offer potential to deliver anticancer drugs for the treatment of Pgp-mediated MDR in leukemia; however, selection of target drug may be very important.

Keywords

solid lipid nanoparticle (SLN); idarubicin; doxorubicin; Pgp; multiple drug resistance (MDR)

*Corresponding author: Russell J. Mumper, Ph.D., John A. McNeill Distinguished Professor, Director, Center for Nanotechnology in Drug Delivery, Division of Molecular Pharmaceutics, 1044 Genetic Medicine Building, CB 7362, 120 Mason Farm Road, University of North Carolina at Chapel Hill, Chapel Hill, North Carolina 27599-7362, mumper@email.unc.edu, Phone: (919) 966-1271, Fax: (919) 966-0197.

INTRODUCTION

Anthracyclines rank among the most effective anticancer drugs ever developed [1]. The cytotoxicity of anthracyclines is generally due to their ability to diffuse across the cell membrane, intercalate between DNA base pairs, and target topoisomerase II [2]. Doxorubicin (DOX, Figure 1A) is one of the oldest anthracyclines and is commonly used to treat leukemia, Hodgkin's lymphoma, bladder and breast cancers. Idarubicin (IDA, 4-demethoxydaunorubicin, Figure 1A), a synthetic analog of daunorubicin (DNR), was approved by the US FDA in 1990. It is mainly used to treat acute myelogenous leukemia (AML) and chronic lymphocytic leukemia (CLL) [3]. The absence of the methoxy group at position 4 of IDA results in significantly enhanced lipophilicity [4], which results in faster cellular uptake, superior DNA-binding capacity, and consequently greater cytotoxicity compared to DOX and DNR.

After initial treatment with anthracyclines, many patients achieve a complete remission; however, about 70% of the patients eventually experience a relapse of the disease. A major cause of treatment failure in patients with leukemia is the development of MDR. Different MDR mechanisms have been characterized [5]. P-glycoprotein (Pgp), a membrane transporter encoded by the MDR1 gene, is responsible for the efflux of anthracyclines used in the treatment of leukemia. Goasguen *et al.* [6] reported the correlation of complete remission, relapse rate and lymphoblast Pgp expression in a study involving 23 adult patients with acute lymphoblastic leukemia (ALL). In this study, complete remission was achieved in 5/9 Pgp+ patients compared to 13/14 of Pgp- patients (56 vs. 93%). During the follow-up period, relapse occurred in all Pgp+ patients that had initially shown complete remission compared to 6/13 Pgp- patients (100% vs. 46%), which indicated that the presence of a critical level of functional Pgp in leukemic lymphoblasts was potentially an important determinant of response to chemotherapy treatment. To overcome Pgp-mediated MDR in leukemia, various Pgp inhibitors, such as quinine, cyclosporine A, and PSC 833, have been developed and co-administered with anticancer agents [7–9]. This approach resulted in significant improvement in anthracycline tumor therapy. However, the co-administration of Pgp inhibitors with anticancer drugs often results in enhanced drug toxicity due to the non-specific inhibition of Pgp that leads to alteration of drug elimination pathways, e.g. in liver or kidney [10].

The use of small particle delivery systems, such as liposomes and nanoparticles (NPs), has been shown experimentally to improve cancer treatment as carriers of conventional chemotherapeutic agents [11]. The utility of nano-scale delivery systems is based on their potential to enhance drug delivery into tumor tissues (e.g. EPR effect), while minimizing systemic exposure and thus enhancing drug efficacy and reducing non-specific toxicity. These colloidal delivery systems have also been shown to increase the circulation time of drugs in the blood, thereby increasing the ability of drugs to reach their sites of action. The efficacy of these systems has been reported utilizing numerous cancer drugs including paclitaxel, tamoxifen, and anthracyclines. For example, Gian and colleagues [12] developed IDA SLNs and determined the pharmacokinetics after duodenal administration in rats. The authors found that duodenally administered SLNs increased IDA exposure and the area under the curve (AUC) of concentration versus time profiles. In addition, the elimination half-life of IDA SLNs was 21-fold and 30-fold higher, respectively, as compared to a solution of free IDA.

SLNs have attracted increasing attention during recent years. The major advantages of these SLNs include high drug loading and entrapment efficiency, improved drug stability, and potential biocompatibility since the SLNs use lipids [13]. Due to the fact that many anthracyclines have cationic moieties, counter-ions have been employed to facilitate the entrapment of the drug in SLNs. The Gasco group [14] showed that either decyl phosphate or hexadecyl phosphate could form ion-pairs with DOX or IDA in SLNs containing stearic acid and egg lecithin. The resulting ion-pair complexes increased the lipophilicity of IDA and DOX,

which resulted in an increase in the apparent partition coefficient between stearic acid and water. SLNs containing these lipophilic ion-pairs carried payloads of DOX and IDA at up to 7% and 8.4% (w/w), respectively. Similarly, an anionic hydrolyzed polymer of epoxidized soybean oil (HPESO) was used by Wong and co-workers [15] to complex with cationic DOX. The resulting complex was then dispersed together with a lipid to form DOX SLNs.

In the present studies, an optimized ion-pairing strategy was performed to entrap IDA and DOX in SLNs. Different counter-ions were employed to ion-pair with IDA or DOX and together incorporated into SLN formulations. The main objectives of these studies were: 1) to investigate and compare IDA SLNs and DOX SLNs against Pgp-mediated MDR *in-vitro* and *in-vivo*; and 2) to test the feasibility of the SLNs as potential drug carriers for MDR-related cancer therapy. IDA and DOX SLNs were engineered from warm microemulsion precursors. The SLN formulations versus free drug solutions were tested in different mouse and human sensitive and Pgp-overexpressing cell lines *in-vitro*, as well as *in-vivo* in NCr-*nu/nu* and CD2F1 mouse models.

MATERIALS AND METHODS

Materials

Idarubicin hydrochloride was obtained from Synbias Pharma Ltd (Donetsk, Ukraine). Doxorubicin hydrochloride, sodium taurodeoxycholate (STDC, >97% pure), dextran sulfate sodium (DS, MWs approx. 5,000 and 8,000), and protease inhibitor cocktail were purchased from Sigma (St. Louis, MO, USA). Emulsifying wax (E-wax), and sodium tetradecyl sulfate (STS) were from Spectrum Chemicals (New Brunswick, NJ, USA). Polyoxyl 20-stearyl ether (Brij 78) was obtained from Uniqema (Wilmington, DE, USA). DSPE-PEG_{3000} (25 mg/mL in chloroform) was purchased from Avanti Polar Lipids (Alabaster, AL, USA). RIPA buffer (containing 25 mM Tris-HCl pH 7.6, 150 mM NaCl, 1% NP-40, 1% sodium deoxycholate, 0.1% SDS), and the bicinchoninic acid protein assay kit were from Thermo Scientific (Rockford, IL, USA). Mouse monoclonal antibody Mdr-1 (D-11), β-actin mouse monoclonal antibody, and goat anti-mouse IgG-HRP were bought from Santa Cruz Biotechnology (Santa Cruz, CA, USA). Vitamin E TPGS was generously provided by Eastman Chemical Co. (Kingsport, TN, USA). Dextran sulfate sodium (MW approx. 2,500) was obtained from ABCR GmbH & Co. (Karlsruhe, Germany).

Human colorectal carcinoma cell line HCT-15, human breast cancer cell line MDA-MB-468, and human promyelocytic leukemia cell line HL-60 were purchased from ATCC (Manassas, VA, USA). The resistant cells HL-60/VCR and HL-60/ADR were kindly provided by Dr. Baer (Roswell Park Cancer Institute, Buffalo, NY, USA). Murine leukemia P388 and P388/ADR cell lines were obtained from the NCI (Frederick, MD, USA). The MDA-MB-468 cell line was maintained in DMEM and all the other cell lines were cultured in RPMI-1640 medium (Invitrogen, Carlsbad, CA, USA) containing 10% fetal bovine serum (FBS) (ATCC, Manassas, VA, USA) and antibiotics at 37°C in 5% CO_2 humidified atmosphere.

Preparation of IDA or DOX Ion-Pair Complex

To neutralize the charges of cationic anthracyclines and enhance drug entrapment, an ion-pair complex was prepared using a co-precipitation method. STDC, dextran sulfate sodium (MWs approx. 2,500, 5,000, and 8,000), and STS were investigated as potential counter-ions. The amount of IDA or DOX used was calculated as the base form throughout the experiments. One hundred (100) μL of 1 mg/mL IDA or DOX in water was aliquoted into a series of 1.5 mL centrifuge tubes, and then 100 μL of different concentrations of ion-pairing aqueous solution was added to the tubes. The tubes were shaken for 5 min with the speed of 40 rpm, and centrifuged for another 5 min with the speed of 1,530 × *g*. The concentrations of IDA or DOX

in the supernatant were measured using a spectrophotometer. The percentage of the drug ion-paired with counter-ions was calculated as follows:

$$\%\ \text{of the drug ion-paired with counter-ions} = [\,100\% - (\%\ \text{drug in supernatant})\,](\text{w/w})$$

Preparation of NPs from Microemulsion Precursors

Microemulsion precursors were prepared as reported by Mumper *et al.* [16]. Briefly, 2 mg of E-wax as the oil phase, 2.3 mg of Brij 78, and 3.0 mg of Vitamin E TPGS as the surfactants were accurately weighed out into a 7 mL glass vial. The vial was heated to 65°C to melt the oil and surfactants while stirring. The IDA or DOX ion-pair complex precipitate was dissolved in ethanol and transferred to the vial containing the oil and surfactant mixture. Residual ethanol was evaporated under a stream of nitrogen gas, and then preheated deionized water was added to obtain a final volume of 1 mL. Oil-in-water microemulsions formed spontaneously at this elevated temperature. Upon direct cooling of the warm microemulsions to room temperature, clear SLN suspensions were formed. Polyethylene glycol coated NPs (PEG NPs) were also engineered as described above, except that 16 μL of a DSPE-PEG_{3000} stock solution in water (10 mg/mL) was added to the vial five min before cooling. Blank NPs were prepared in the same manner except that the IDA or DOX, and ion-pairing agents were omitted.

Characterization of NP Formulations

Photon Correlation Spectroscopy—The average particle size and polydispersity index (PI) of IDA or DOX NPs were determined by photon correlation spectroscopy (PCS) using a Coulter N5 Plus Sub-Micron Particle Sizer (Beckman Coulter, Miami, FL, USA) at a fixed angle of 90° and a temperature of 25°C. Prior to size determination, NP suspensions were diluted in deionized water to ensure light scattering intensity within the required range of the instrument (5×10^4 to 1×10^6 counts/s). Each sample was analyzed in triplicate.

Zeta Potential Determination—To determine the zeta potential, NP samples were diluted 1:100 (v/v) with 10 mM PBS (pH 7.4) and placed in the dip cell of Zetasizer Nano Z (Malvern Instruments, Westborough, MA, USA). Each sample was analyzed in quintuplicate.

% Entrapment of NPs—To determine % entrapment of IDA or DOX in the NPs, Microcon Ultracel YM-100 Centrifugal Filtration Devices (MW cut-off 100 kDa) (Millipore, Billerica, MA, USA) were used. A fixed volume (300 μL) of the drug NP formulations was added to a Microcon tube and spun at 14,000 × *g* at 25°C for 30 min. The collected filtrate in the tube was labeled as “free drug filtrate”. Then the filter apparatus was removed, inverted, and transferred to a new Microcon tube. Drug NPs were spun at 6,000 × *g* at 25°C for 4 min and collected in this tube labeled as “drug in NPs”. Concentrations of IDA or DOX were determined using a Synergy 2 Multi-Detection Microplate Reader (BioTek, Winooski, VT, USA) at the wavelengths of 483 and 487 nm, respectively. The % entrapment was calculated as follows:

$$\%\ \text{entrapment} = [\,(\text{mass of drug in NPs})/(\text{mass of drug added into NP formulations})\,] \times 100\%\ (\text{w/w})$$

Western Blot Analysis

Cellular content of the Mdr-1/Pgp transporter molecule was detected by western blot analysis in P388, P388/ADR, and HCT-15 cell lines. Briefly, 10^7 cells were lysed in 0.3 mL RIPA buffer, including protease inhibitor cocktail. The quantification of the protein content was performed with the bicinchoninic acid (BCA) protein assay kit. For immunoblotting, 40–60 μg of total protein extract was mixed with Laemmli sample buffer (Bio-Rad Laboratories,

Hercules, CA, USA) and transferred to a 10% polyacrylamide gel. Gel electrophoresis was performed with a Mini Protean® 3 Cell (Bio-Rad Laboratories, Hercules, CA, USA) applying 100V for 100 min. After electrophoresis, proteins were blotted to a PVDF membrane (100V for 1 hr) using a Mini Trans-Blot® Cell (Bio-Rad Laboratories, Hercules, CA, USA). The membrane was blocked for 1 hr with PBS-T (phosphate buffered saline containing 0.05% Tween 20) with 5% nonfat milk. After washing three times with PBS-T, the membrane was incubated at 4 °C overnight with the primary mouse monoclonal antibody Mdr-1, diluted 1:200 (v/v) in PBS-T with 5% nonfat milk. β-actin was used as a loading control by staining with β-actin mouse monoclonal antibody at a dilution of 1:2000 (v/v). After incubation with the first antibody, the membrane was washed with PBS-T three times and then incubated with the secondary goat anti-mouse IgG-HRP diluted 1:2000 (v/v) for 1 hr at room temperature. The membrane was then washed, and Pgp and β-actin detection were performed with the ECL Detection VersaDoc™ Imaging System (Bio-Rad Laboratories, Hercules, CA, USA). The molecular weight was identified using the Precision Plus Protein™ Standard Dual Color (Bio-Rad Laboratories, Hercules, CA, USA).

In-Vitro Cytotoxicity Assay

The MTT (3-[4,5-dimethylthiazol-2-yl]-2,5-diphenyl tetrazolium bromide) assay was utilized to assess cytotoxicity of the NPs [17]. Viable cells were counted by trypan blue staining (>90% cell viability for experiments) and seeded in 96-well plates at 8,000 cells/100 μL growth medium. Serial dilutions of DOX or IDA formulations were added to the plate (100 μL/well) at 37°C in 5% CO_2 for 48 hr. The cells were then incubated with MTT stock solution (5 mg/mL in PBS; pH 7.4) at 37°C for 4 hr. Cell suspensions were spun down for 10 min at 1,000 × *g* (this step was not required for adherent cell lines). The medium was then removed and the converted dye was solubilized with the addition of DMSO. The absorbance was measured using the Synergy 2 Multi-Detection Microplate Reader at 570 nm, and the concentration of drug that inhibited cell survival by 50% (IC_{50}) was determined from cell survival plots.

Cellular Uptake of Free IDA and IDA NPs

Cellular uptake of free IDA and IDA NPs were performed in HL-60 and HL-60/VCR cell lines. Different dilutions of each test article were added to a 12-well plate (7.5×10^5 cells/well). After 4 hr incubation at 37°C in 5% CO_2, cells were transferred to 15 mL graduated tubes and centrifuged. The medium was then aspirated and replaced with fresh medium. Cell-associated fluorescence was read using the Synergy 2 Multi-Detection Microplate Reader at the excitation and emission wavelengths of 485 ± 20 and 545 ± 10 nm, respectively.

Visualizing Cellular Uptake of IDA and DOX NPs

MDA-MB-468 cells were first plated onto glass slides, then aliquots of free DOX or IDA, and their NPs (10 μL) were dispersed on glass slides and covered with coverslips. The cellular uptake of free drug and drug NPs was visualized with CytoViva Microscope System (Auburn, AL) at room temperature.

In-Vivo Animal Efficacy Studies

Five-week-old male CD2F1 or six-week-old male athymic NCr-*nu/nu* mice from NCI-Frederick Animal Production Area (Frederick, MD, USA) were used for the studies. All mice were on a 12-hr light/dark cycle and sterilized rodent diet (Harlan-Teklad TD8656) *ad libitum*. The animal experiments complied with the rules set forth in the NIH Guide for the Care and Use of Laboratory Animals. In total, three separate *in-vivo* studies were performed; the first two studies using IDA formulations and the third study using DOX formulations.

Study 1 was to treat with free IDA and IDA NPs in male athymic nude mice which were subcutaneously (s.c.) implanted with HCT-15 human colon tumor cells. Study 1 consisted of a vehicle-treated control group (saline) having 10 mice, and 9 treatment groups with 10 mice each for a total of 100 mice. Free IDA and IDA-STS PEG NPs were administered intravenously (i.v.) at doses of 2.25, 1.5, 1.0, and 0.67 mg/kg/injection on a q4d × 3 treatment schedule. Study 2 was designed to treat with free IDA and IDA NPs in male CD2F1 mice which were i.v. implanted with P388 murine leukemia cells. Study 2 consisted of a vehicle-treated control group (saline) having 10 mice, and 12 treatment groups with 6 mice each for a total of 82 mice. Free IDA, IDA-STS NPs and IDA-STS PEG NPs were each i.v. injected at doses of 2.25, 1.5, 1.0, and 0.67 mg/kg/injection on a q4d × 3 treatment schedule. The experimental procedures of studies 1–2 were similar to the following study 3 of DOX formulations.

Study 3 was designed to treat with free DOX and DOX NPs in male CD2F1 mice in which 10^5 P388/ADR murine leukemia cells were implanted intraperitoneally (i.p). The day of tumor cell inoculation was designated as Day 0. The animals were randomly assigned to the various treatment groups on Day 1 after tumor implantation. The experiment consisted of a vehicle-treated control (saline) having 10 mice, and 12 treatment groups with 6 mice each for a total of 82 mice at the start of treatment on Day 1. Free DOX, DOX NPs, DOX PEG NPs, and blank NPs were each injected i.p. at doses of 8.0, 5.3, and 3.5 mg/kg/injection on a q4d × 3 treatment schedule. Doses were administered by exact body weight using an injection volume of 0.1 mL/10 g of body weight. The number of 25 day survivors, median day of death, and Increase in Life-Span (ILS) based on median day of death were recorded. The percentage of ILS was calculated as follows:

$$\%\,\mathrm{ILS} = [\,(\text{median death time of a treatment group} - \text{median death time of the control group})/(\text{median death time of the control group})\,] \times 100\%$$

Statistical Analysis

For the animal efficacy studies, statistical analysis was conducted using a life table analysis (stratified Kaplan-Meier estimation followed by the Mantel-Haenszel log-rank test). A life table analysis allowed the data between groups using the animals that did not reach the endpoint to be compared by censoring them. When appropriate, the data sets were analyzed using Student's t-test. Differences were considered significant if $p < 0.05$.

RESULTS

Preparation of IDA Ion-Pair Complex

To facilitate the entrapment of positively charged IDA or DOX in the oil phase, several negatively charged ion-pairing agents were identified and tested, such as STDC, DS2500, DS5000, DS8000, and STS. Figure 2 shows the % IDA ion-paired with STS at different IDA/STS molar ratios in aqueous solution. At IDA and STS molar ratios of 1:2, 1:1.75, 1:1.5, and 1:1.25, greater than 95% of IDA was ion-paired with STS. As more or less STS were added, the % IDA formed in ion-pair complex decreased as indicated by the bell-shaped curve. The optimal IDA/STS molar ratio was 1:1.25, at which 98.0 ± 0.1% of IDA ion-paired with STS. Therefore, this IDA/STS molar ratio was used for future IDA-STS NP preparations. Figure 1B displays the structure of the IDA-STS or DOX-STS complex. The negatively charged sulfate group on STS attracts the positively charged amino sugar moiety on IDA or DOX in roughly a 1:1 molar ratio. Furthermore, the long alkyl chain on STS increases the lipophilicity of the complex thereby facilitating the entrapment of IDA or DOX in the oil phase. The optimal weight ratios of IDA/DS2500, IDA/DS5000, IDA/D8000 were 2.94:1, 3.48:1, 2.49:1, respctively, at which more than 90% IDA ion-paired with all various DS counter-ions.

However, probably due to the large size of the DS molecule and its relative hydrophilicity, the loading of the IDA-DS or DOX-DS ion-pair complex in the oil phase was low. The optimal IDA/STDC molar ratio was 1:1. Therefore, STDC and STS were selected as ion-pairing agents in our studies. The optimal molar ratio of DOX and STS was 1:1.25 (data not shown).

Characterization of NP Formulations

Table 1 reports the average particle size, PI, % entrapment, and zeta potential values for IDA and DOX NPs. The average particle size of either IDA NPs or DOX NPs was less than or around 100 nm. PI values were small (< 0.3) indicating uniform and mono-disperse NP suspensions. Entrapment efficiencies were also high (> 80%) and zeta potential ranged from −5 to −15 mV.

More concentrated IDA-STDC NPs, from 240 μg up to 600 μg IDA/mL, were also successfully engineered by simply decreasing the volume of aqueous phase in the warm o/w microemulsion while keeping the composition of oil phase (oil + surfactant + drug) constant (Figure 3). No significant changes of particle size and PI values were observed between different concentrated NP formulations. This provides a very convenient method for preparing concentrated NP preparations by simple adding less water during the formation of the warm oil-in-water microemulsions. In a similar manner, DOX-STS NPs could also be prepared from 200 μg up to 800 μg DOX/mL without significant change in particle size and PI values (data not shown).

Western Blot Analysis

Expression of Pgp levels in P388, P388/ADR, and HCT-15 cell lines was detected using western blot analysis. As shown in Figure 4, P388/ADR and HCT-15 cell lines overexpressed Pgp, while P388 cells did not demonstrate any Pgp-specific signal. This was consistent with the documented information on Pgp expression level for these cell lines. β-actin was used as the loading control. The Pgp expressions of P388/ADR and HCT-15 cells were comparable when normalized to β-actin.

In-Vitro Cytotoxicity Assay

In-vitro cytotoxicity of free IDA or free DOX, IDA NPs or DOX NPs, and blank NPs were conducted in various sensitive and resistant cell lines. The IC_{50} values of different IDA or DOX formulations are listed in Table 2. IDA NPs showed comparable cytotoxicity with free IDA in most of the cell lines tested. In some resistant cell lines (e.g. P388/ADR), although the difference in IC_{50} values was statistically significant, the cytotoxicity of IDA NPs was only 1–2 fold lower than that of free IDA. In contrast, the IC_{50} values of DOX NPs were almost 10-fold lower than that of free DOX in P388/ADR cell line. In the sensitive cell line P388, DOX NPs showed equivalent cytotoxicity to free DOX as expected ($p = 0.13$). Blank NPs were shown to be cytotoxic when the drug equivalent NP concentration was about 1000 nM.

Cellular Uptake of Free IDA and IDA NPs

Cellular uptake of free IDA and IDA NPs were performed in both sensitive HL-60 and resistant HL-60/VCR cell lines. After a period of 4 hr incubation, a concentration dependent increase in the cell-associated fluorescence intensity was observed for both free IDA and IDA NPs in both cell lines (Figure 5). There was little or no difference between free IDA and IDA NPs within each cell line. More notably, there was no or little statistical difference in the cell-associated fluorescence for free IDA and IDA NPs between the HL-60 (Figure 5A) and HL-60/VCR (Figure 5B). For example, at an IDA concentration of 25 nM, the cell-associated fluorescence intensity of free IDA and IDA NPs was 75 ± 5 and 115 ± 42 in HL-60, respectively, and 98 ± 7 and 180 ± 32 in HL-60/VCR, respectively. These data suggest that free IDA may not be strongly effluxed from the Pgp-overexpressing HL-60/VCR cell line. This is in sharp

contrast to our previous studies in Pgp-overexpressing human ovarian carcinoma NCI/ADR-RES cell line, wherein greater than 15-fold DOX remained in the Pgp cells for DOX NPs as compared to free DOX after 4 hr of efflux [18].

Visualizing Cellular Uptake of IDA or DOX NPs

Cell uptake of free IDA and DOX, and their NPs were visualized with the CytoViva Microscope System. The uptake rate of free IDA was faster than that of free DOX, which is due to its higher lipophilicity. The extent and rate of uptake for both NP formulations was high as after 10 min, significant red fluorescence of DOX was seen in most of the nuclei in MDA-MB-468 cells. However, and in stark contrast, the fluorescence of IDA was seen every where in the cell except the nucleus (Figure 6).

In-Vivo Animal Efficacy Studies

In study 1, the treatment with free IDA and IDA NPs were ineffective in inhibiting the growth of the HCT-15 human colon tumor cells at the lower doses of 1.0 and 0.67 mg/kg/injection. At higher doses of 2.25 and 1.5 mg/kg/injection, both free IDA and IDA NPs treatment resulted in more than five of ten mice death within 27 days. In the study 2, free IDA and IDA-STS NPs, and free IDA and IDA-STS PEG NPs were equally effective against the P388 murine leukemia in CD2F1 mice when administered i.v. at doses of 1.5 and 1.0 mg/kg/injection. At the higher dose of 2.25 mg/kg/injection, the maximum losses in average body weight of the mice were 16.1% (3.7 g) and 26.5% (6.3 g), respectively, in free IDA and IDA-STS PEG NPs treatment groups. At the lower dose of 0.67 mg/kg/injection, the difference in survival time between free IDA and IDA-STS NPs treatment was only one day (data not shown).

In the study 3, the % ILS after i.p. treatment with DOX NPs was found to be statistically significant when compared with DOX PEG NPs, blank NPs, and free DOX in the P388/ADR murine leukemia model in male CD2F1 mice at dose of 3.5 mg/kg/injection given with the treatment schedule of q4d×3 (Figure 7). This treatment resulted in a median day of death of 20 days and ILS value of 67% for DOX NPs, 16.5 days and 38% for DOX PEG NPs, 14.5 days and 21% for free DOX, and 11 days and −8% for blank NPs, respectively. DOX PEG NPs and free DOX were equally effective, and as expected, treatment with blank NPs was ineffective. At dose of 5.3 mg/kg/injection, DOX NPs was found to be statistically significant when compared with blank NPs ($p = 0.0497$), or approached statistically significant compared with DOX PEG NPs ($p= 0.0835$); while at dose of 8.0 mg/kg/injection, there was no survival difference between DOX NPs and the other groups, and the median day of death for all groups ranged from 12.5 to 14.5 days.

DISCUSSION

In the present study, IDA NPs and DOX NPs were engineered using a microemulsion precursor method previously described by the Mumper group [19]. This method provides many advantages including formulation adaptability to several different excipients, reproducibly engineered and well defined solid NPs (<100 nm), and no need for expensive and/or damaging high-torque mechanical mixing, microfluidization, or homogenization. Emulsifying wax, Brij 78, Vitamin E TPGS and together with the ion-pairing complex were utilized to form a warm oil-in-water microemulsion precursor, which solidified to SLNs upon direct cooling. This microemulsion precursor method allowed instantaneous and reproducible formation of both IDA and DOX NPs, with exhibited diameters around or below 100 nm, small PI (< 0.3), high entrapment efficiency (> 80%) and homogenous size distribution. The zeta potential of both SLNs was slightly negative, range from −5 to −15 mV. A 15-day physical stability test of the IDA NPs at 4°C was also conducted and no statistical difference was found when comparing the particle size over time (data not shown).

Particle size is a very important parameter for characterizing the physicochemical properties of SLNs. Since NPs with large size will usually be taken up by liver, spleen and other parts of the reticuloendothelial system (RES) *in-vivo*, particles with size less than 100 nm in diameter and a uniform size distribution are preferred for tumor targeting [20]. In addition to particle size, particle surface properties will also affect particle uptake route [21]. Since NPs with more hydrophobic surface will preferentially be taken up by liver, followed by spleen and lungs, presentation of a more hydrophilic surface is desired [22]. Therefore, insertion of hydrophilic PEG groups on the surface is a common strategy to enhance the hydrophilicity of the particle surface [23]. In our study, DOX PEG NPs were prepared to enhance *in-vivo* performance. However, the results showed that DOX PEG NPs were less effective in ILS than non-pegylated DOX NPs in the P388/ADR CD2F1 mouse model, which may be due to reduced cell uptake of the pegylated formulation (Figure 7).

To neutralize the cationic charge and enhance entrapment of IDA and DOX hydrochloride salt forms, counter-ions such as STDC and STS were employed. STDC and STS were effective counter-ions for IDA and DOX in our SLN formulations. Titration of an aqueous solution of IDA or DOX with aqueous solution of STDC or STS resulted in immediate formation of ion-pair complex as red precipitates. During this complexation process, more than 95% of the drugs could ion-pair with counter-ions, which was very efficient. The obtained ion-paired precipitate was isolated by centrifugation and was soluble in ethanol. This counter-ion strategy was also employed previously by the Gasco group [14]. The Gasco group used decyl phosphate or hexadecyl phosphate to form ion-pairs with DOX or IDA hydrochloride and increase the entrapment of these drugs in SLNs. Although the group achieved a relatively high loading of IDA and DOX up to 7% and 8.4% (w/w) and low drug release rate (0.1% in 2 hr) when the SLNs were placed in water, however, ideally the release study should be performed in PBS instead of water, which is biologically more relevant and also provides the necessary pH and ionic strength to test the ability of the ion-pairing agent to retain the drug in the SLNs. The IDA and DOX SLNs in the present studies had a loading capacity up to 10% (w/w), and the release rate for IDA and DOX from NPs made with STDC as the ion-pairing agent was 100% in 6 hr in PBS at 37°C. In contrast, the release rate for DOX from NPs made with STS as the ion-pairing agent was 84% in 24 hr (data not shown). The slower release rate of drug from NPs made with STS as the ion-pairing agent is most likely due to the enhanced stability of the STS ion-pair complex in PBS as compared to the STDC ion-pair complex.

IDA or DOX SLNs have also been formulated to address Pgp-mediated MDR by several other research groups. Wong *et al.* [15] prepared DOX SLNs with a drug entrapment efficiency of 60–80% and particle size ranging from 80–350 nm. Treatment of MDR cells with their DOX SLNs resulted in an over 8-fold increase in cell death when compared to DOX solution treatment at equivalent doses. In comparison, the DOX NPs in the present studies had increased entrapment efficiency, smaller and more monodisperse particle size, and almost a 10-fold greater cytotoxicity in a Pgp-overexpressing cell line P388/ADR. Furthermore, at the dosage of 3.5 mg/kg/injection to our P388/ADR mouse model, the median survival time was 20 days after DOX NP treatment and only 14.5 days after free DOX treatment, which significantly improved therapeutic effect in this MDR mouse model. In sharp contrast, IDA NPs showed comparable cytotoxicity with free IDA in most of the cell lines tested *in-vitro*. IDA NPs were also equally effective as free IDA *in-vivo* in P388 mouse model and ineffective *in-vivo* in HCT-15 mouse model. The Pgp expression in P388/ADR and HCT-15 cells and lack thereof in P388 cells was confirmed by western blot analysis (Figure 4). Our findings are in agreement with the previous report from Nancy and co-workers [17]. The authors formulated IDA liposomes to improve its antitumor activity. However, the results demonstrated that neither free IDA nor the IDA liposome formulation was therapeutically active *in-vivo* in resistant P388/ADR or MDA435LCC6/MDR1 models.

The mechanism responsible for the different cytotoxic activity of IDA NPs and DOX NPs versus free drug observed in Pgp-overexpressing cells both *in-vitro* and *in-vivo* remains to be addressed, although the models applied were different (HCT-15 cell model for IDA and P388/ADR cell model for DOX, respectively). The compositions of excipients in both NP formulations were the same except for very slight differences in the amount of the ion-pairing agent used in the formulations. Both IDA and DOX belong to the anthracycline family and have the same amino sugar moiety, daunosamine, with a pKa of 8.4, which bears the positive electrostatic charge localized at the protonated amino nitrogen. Thus, both drugs should exhibit similar electrostatic interactions with cell membrane [4]. However, IDA has a hydrogen atom in position 14, where DOX has a hydroxyl group attached. Furthermore, IDA does not have the methoxy group at position 4 (Figure 1A), which results in significantly increased lipophilicity and cell permeability as compared with DOX [24].

The molecular mechanism of IDA action does not seem to differ significantly from that of DOX. Both drugs accumulate in the nucleus and intercalate into DNA, which seems to be the main locus of activity. However, another interesting finding in these studies was the difference in the intracellular localization of IDA and DOX in sensitive cells after 10 min. Whereas IDA was found largely extra-nuclear after 10 min, DOX was almost entirely intranuclear. This observation was supported by Zohreh *et al.* [25], who found the binding affinity of DOX to chromatin was higher than that of IDA; therefore, higher aggregation of chromatin with DOX occurred. They also suggested that the weaker interaction of IDA with chromatin is possibly attributed to its higher lipophilic nature.

It should be kept in mind that the activity of a drug depends largely upon its intracellular concentration, and specifically for IDA and DOX the nuclear concentration, which is basically determined by the kinetics of its influx and efflux of the drug across cell membrane. The influx rate is greatly affected by the lipophilicity of the drug, while the efflux rate is correlated with Pgp and MRP associated MDR. Marbeuf-Gueye *et al.* [26] have demonstrated that the relative drug resistance of anthracyclines poorly correlated with drug efflux kinetics in Pgp-expressing cells, which indicates that the influx rate may be the more important contributor to the intracellular concentration for anthracyclines. The IDA cell uptake studies in both sensitive HL-60 and resistant HL-60/VCR cell lines demonstrated that the cellular uptake of IDA was comparable for both IDA NPs and free IDA. In addition, no significant difference in the cellular uptake of IDA was found between the sensitive and resistant cell lines (Figure 5), which suggests that the increased lipophilicity of IDA may help circumvent MDR by the influx-governed mechanism and thereby enhance its chemotherapeutic efficacy. Similar results were previously reported by Carole *et al.* [27]. They demonstrated that the uptake rate of IDA was much higher than the efflux rate mediated by Pgp, which may be a main factor in the improved IDA cytotoxicity observed in MDR cells *in-vitro*. In contrast, after treatment of Pgp-overexpressing human ovarian carcinoma cell line NCI/ADR-RES with our DOX-STS NPs, greater than 15-fold DOX remained in the Pgp cells compared to free DOX [18]. The mechanism responsible for increased cellular uptake of our DOX SLNs may be mediated by the endocytosis pathway described earlier [10]. Wong *et al.* [15] also proposed two possible mechanisms of cytotoxicity for DOX SLNs: 1) DOX is released from DOX SLNs outside the cells and works like free DOX, but its cytotoxicity is enhanced by NPs; 2) DOX is carried by NPs into the cells and released inside the cells, resulting in higher cytotoxicity. They also suggested that the mechanisms of SLNs responsible for reversal of MDR activities are diversified and probably vary from one drug carrier to another. Since Pgp efflux is an energy dependent process, intracellular ATP levels were also investigated. In previously studies by our group, it was found that the surfactants Brij 78 and Vitamin E TPGS inhibited Pgp (as evidenced by increased calcein AM influx), but only Brij 78 depleted ATP [18]. It also should be noted that cell nucleus is the major target of anthracyclines, and it has been demonstrated that the nuclear membrane also expresses Pgp to prevent drug penetration into the cell nuclei

[28]. SLNs may be able to overcome this possible source of drug resistance as well, although the mechanism is not fully understood.

CONCLUSIONS

The engineered IDA and DOX SLNs from warm microemulsion precursors were manufactured in a one-vessel procedure that does not require high-torque mechanical mixing, and were physically stable with diameters of less than 100 nm at least over 15 days stored at 4°C. *In-vitro* cytotoxicity studies revealed that the IC_{50} value of DOX NPs was almost 10-fold lower than that of free DOX in resistant P388/ADR cells ($p = 0.01$), whereas IDA NPs had comparable IC_{50} values as free IDA in all the cell lines tested. In the *in-vivo* P388/ADR leukemia mouse model, at the dose level of 3.5 mg/kg, the median survival time of DOX NPs was 20 days, which was significantly higher than that of free DOX (14.5 days), or untreated or placebo NPs (11 days). However, free IDA and IDA NPs were equally effective in P388 leukemia *in-vivo* mouse model, as well as in HCT-15 *in-vivo* mouse model. Unlike free DOX, free IDA remained active against various Pgp-overexpressing cell lines. This is probably due to the more lipophilic properties of IDA which allows greater cell accumulation and retention of IDA. The present studies show that our SLNs may offer potential to deliver anticancer drugs for the treatment of Pgp-mediated MDR in leukemia; however, selection of target drug may be very important.

Acknowledgments

This research was supported, in part, by NIH-NCI R01 CA115197 to RJM. Dr. Mumper owns stock in NanoMed Pharmaceuticals that provided funding, in part, to support the *in-vivo* studies in this paper.

REFERENCES

1. Weiss RB. The anthracyclines: will we ever find a better doxorubicin? Semin. Oncol 1992;19:670–686. [PubMed: 1462166]
2. Minotti G, Menna P, Salvatorelli E, Cairo G, Gianni L. Anthracyclines: molecular advances and pharmacologic developments in antitumor activity and cardiotoxicity. Pharmacol. Rev 2004;56:185–229. [PubMed: 15169927]
3. Blasiak J, Gloc E, Wozniak K, Mlynarski W, Stolarska M, Skorski T, Majsterek I. Genotoxicity of idarubicin and its modulation by vitamins C and E and amifostine. Chem. Biol. Interact 2002;140:1–18. [PubMed: 12044557]
4. Gallois L, Fiallo M, Suillerot AG. Comparison of the interaction of doxorubicin, daunorubicin, idarubicin and idarubicinol with large unilamellar vesicles circular dichroism study. Biochim. Biophys Acta 1998;1370:31–40. [PubMed: 9518541]
5. Nielsen D, Maare C, Skovsgaard T. Cellular resistance to anthracyclines. Gen. Pharmacol 1996;27:251–255. [PubMed: 8919638]
6. Goasguen JE, Dossot JM, Fardel O, Mee FL, Gall EL, Leblay R, LePrise PY, Chaperon J, Fauchet R. Expression of the multidrug resistance-associated P-glycoprotein (P-170) in 59 cases of *de novo* acute lymphoblastic leukemia: prognostic implications. Blood 1993;81:2394–2398. [PubMed: 8097634]
7. Hayeshi R, Masimirembwa C, Mukanganyama S, Ungell AL. The potential inhibitory effect of antiparasitic drugs and natural products on P-glycoprotein mediated efflux. Eur J Pharm Sci 2006;29:70–81. [PubMed: 16846720]
8. Hamilton KO, Backstrom G, Yazdanian MA, Audus KL. P-glycoprotein efflux pump expression and activity in Calu-3 cells. J Pharm Sci 2001;90:647–658. [PubMed: 11288109]
9. Bauer KS, Karp JE, Garimella TS, Wu S, Tan M, Ross DD. A phase I and pharmacologic study of idarubicin, cytarabine, etoposide, and the multidrug resistance protein (MDR1/Pgp) inhibitor PSC-833 in patients with refractory leukemia. Leuk Res 2005;29:263–271. [PubMed: 15661261]
10. Koziara JM, Whisman TR, Tseng MT, Mumper RJ. In-vitro efficacy of novel paclitaxel nanoparticles in paclitaxel-resistant human colorectal tumors. J Control Release 2006;112:312–319. [PubMed: 16626835]

11. Dutta RC. Drug carriers in pharmaceutical design: promises and progress. Curr. Pharm. Des 2007;13:761–769. [PubMed: 17346190]
12. Zara GP, Bargoni A, Cavalli R, Fundarq A, Vighetto D, Gasco MR. Pharmacokinetics and tissue distribution of idarubicin-loaded solid lipid nanoparticles after duodenal administration to rats. J. Pharm. Sci 2002;91:1324–1333. [PubMed: 11977108]
13. Soukharev AR. Stability of lipid excipients in solid lipid nanoparticles. Adv. Drug Deliv. Rev 2007;59:411–418. [PubMed: 17553589]
14. Cavalli R, Caputo O, Gasco MR. Solid lipospheres of doxorubicin and idarubicin. Int. J. Pharm 1993;89:R9–R12.
15. Wong HL, Rauth AM, Bendayan R, Manias JL, Ramaswamy M, Liu Z, Erhan SZ, Wu XY. A new polymer-lipid hybrid nanoparticle system increases cytotoxicity of doxorubicin against multidrug resistant human breast cancer cell. Pharm. Res 2006;23:1574–1585. [PubMed: 16786442]
16. Oyewumi MO, Mumper RJ. Gadolinium-loaded nanoparticles engineered from microemulsion templates. Drug Dev Ind Pharm 2002;28:317–328. [PubMed: 12026224]
17. Santos ND, Waterhouse D, Masin D, Tardi PG, Karlsson G, Edwards K, Bally MB. Substantial increases in idarubicin plasma concentration by liposome encapsulation mediates improved antitumor activity. J Control Release 2005;105:89–105. [PubMed: 15878792]
18. Dong X, Mattingly CA, Tseng M, Cho M, Adams VR, Mumper RJ. Doxorubicin and paclitaxel-loaded lipid-based nanoparticles overcome multi-drug resistance by inhibiting P-gp and ATP depletion. (Submitted).
19. Hsu C, Cui Z, Mumper RJ, Jay M. Preparation and characterization of novel coenzyme Q10 nanoparticles engineered from microemulsion Precursors. AAPS PharmSciTech 2003;4:32. Article.
20. Peppas LB, Blanchette JO. Nanoparticle and targeted systems for cancer therapy. Adv. Drug Deliv. Rev 2004;56:1649–1659. [PubMed: 15350294]
21. Otsuka H, Nagasaki Y, Kataoka K. PEGylated nanoparticles for biological and pharmaceutical applications. Adv. Drug Deliv. Rev 2003;55:403–419. [PubMed: 12628324]
22. Storm G, Belliot SO, Daemen T, Lasic D. Surface modification of nanoparticles to oppose uptake by the mononuclear phagocyte system. Adv. Drug Deliv. Rev 1995;17:31–48.
23. Oyewumi MO, Yokel RA, Jay M, Coakley T, Mumper RJ. Comparison of cell uptake, biodistribution and tumor retention of folate-coated and PEG-coated gadolinium nanoparticles in tumor-bearing mice. J Control Release 2004;95:613–626. [PubMed: 15023471]
24. Marczak A, Kowalczyk A, Kus AW, Robak T, Jozwiak Z. Interaction of doxorubicin and idarubicin with red blood cells from acute myeloid leukemia patients. Cell Biol. Int 2006;30:127–132. [PubMed: 16271486]
25. Zahraei Z, Chadegani AR. A comparison of the effect of anticancer drugs, idarubicin and adriamycin, on soluble chromatin. Eur. J. Pharmacol 2007;575:28–33. [PubMed: 17716648]
26. Gueye CM, Broxterman HJ, Dubru F, Priebe W, Suillerot AG. Kinetics of anthracycline efflux from multidrug resistance protein-expressing cancer cells compared with P-glycoprotein-expressing cancer cells. Mol. Pharmacol 1998;53:141–147. [PubMed: 9443942]
27. Gueye CM, Ettori D, Priebe W, Kozlowski H, Suillerot AG. Correlation between the kinetics of anthracycline uptake and the resistance factor in cancer cells expressing the multidrug resistance protein or the P-glycoprotein. Biochim. Biophys. Acta 1999;1450:374–384. [PubMed: 10395948]
28. Baldini N, Scotlandi K, Serra M, Shikita T, Zini N, Ognibene A, Santi S, Ferracini R, Maraldi NM. Nuclear immunolocalization of P-glycoprotein in multidrug-resistant cell lines showing similar mechanisms of doxorubicin distribution. Eur. J. Cell Biol 1995;68:226–239. [PubMed: 8603675]

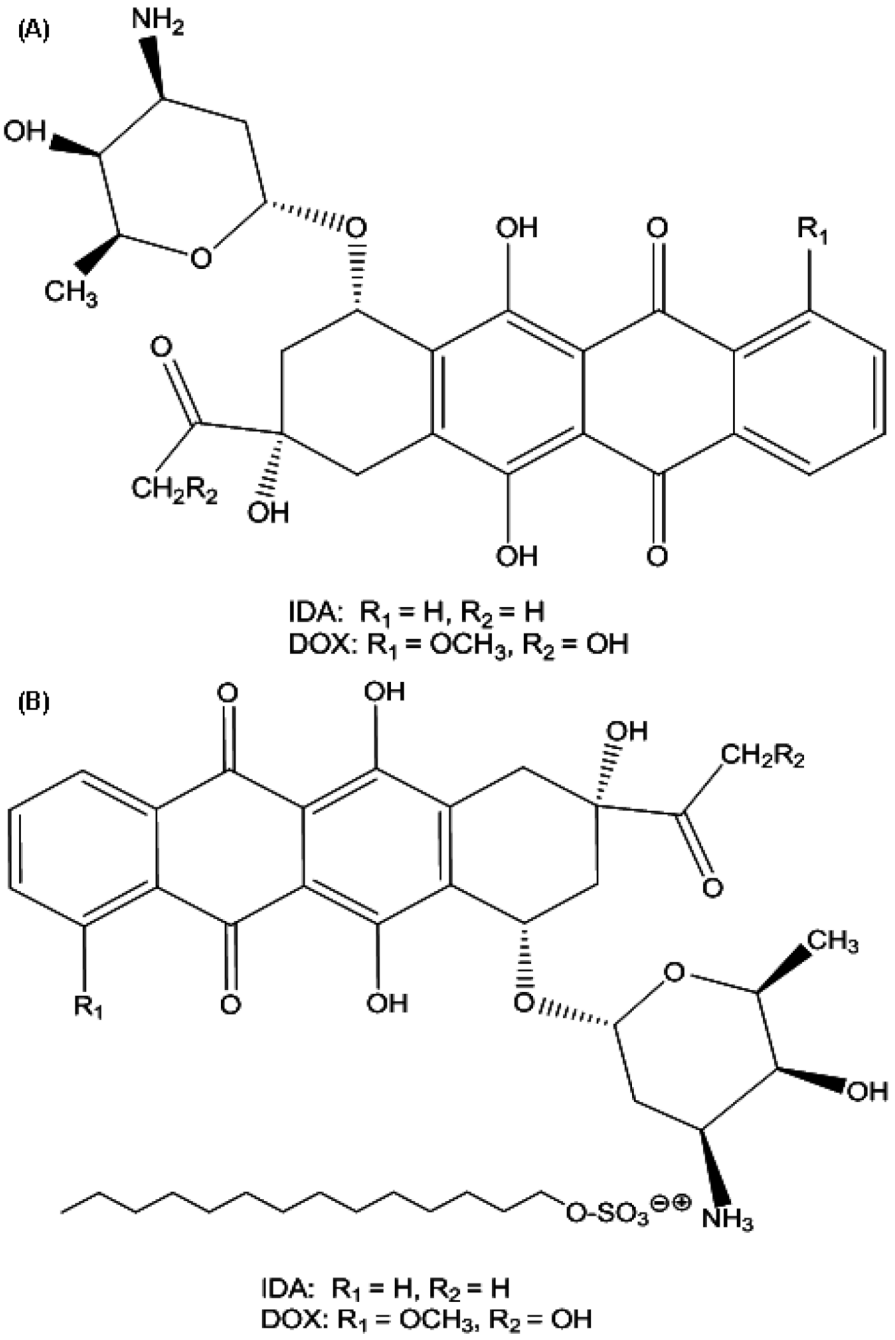

Figure 1.
Chemical structures of (A) IDA and DOX and; (B) the IDA-STS and DOX-STS complexes.

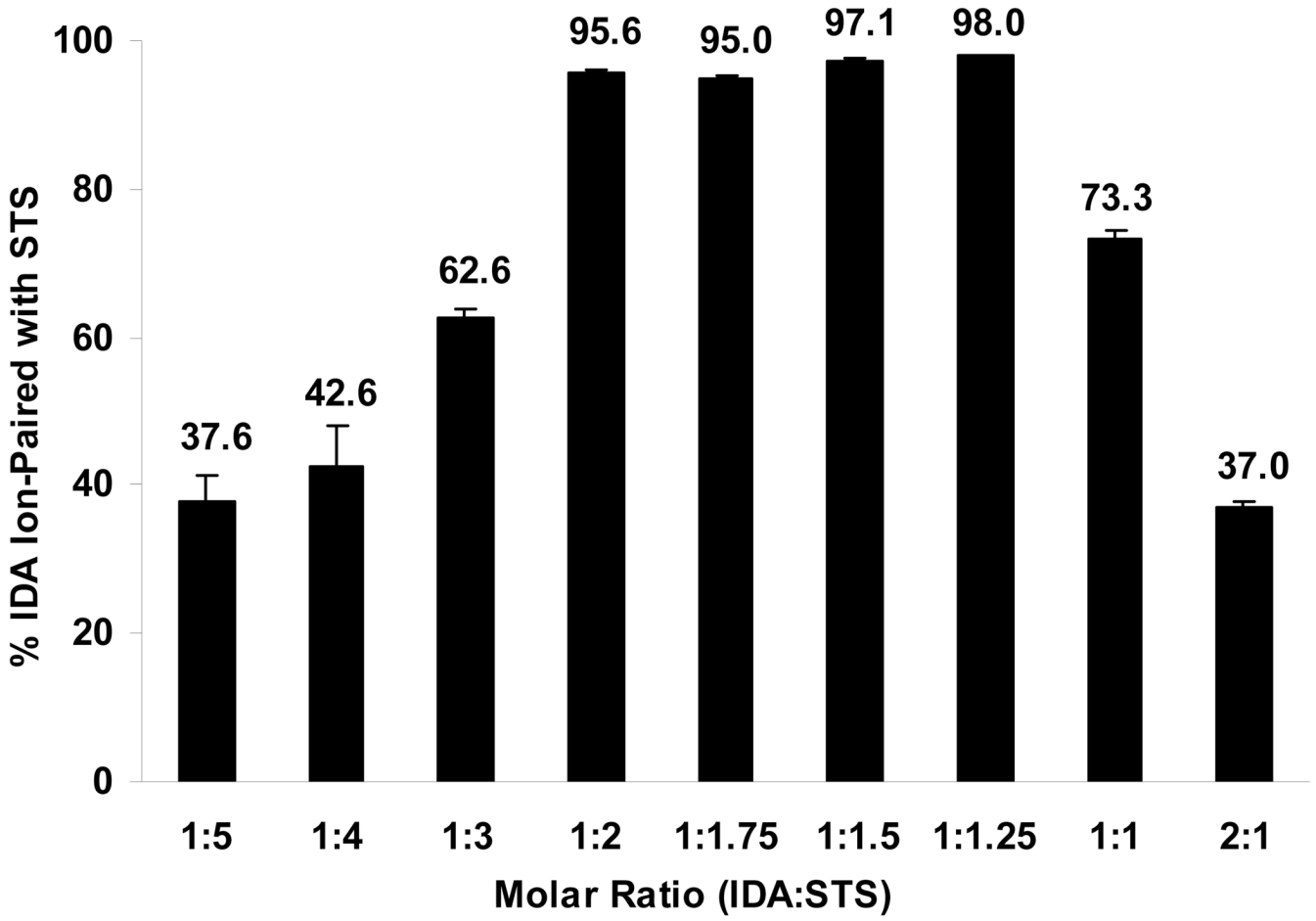

Figure 2.

IDA-STS ion-pair complex formation upon mixing of IDA and STS aqueous solutions. IDA ion-pair complex precipitates were formed upon mixing different molar ratios of IDA and STS aqueous solutions. After precipitation, the ion-pair complex was centrifuged, and the concentrations of IDA in the supernatants were measured. The % of IDA ion-paired with STS was calculated as described in the Methods section. Results are expressed as mean ± SD (n = 3).

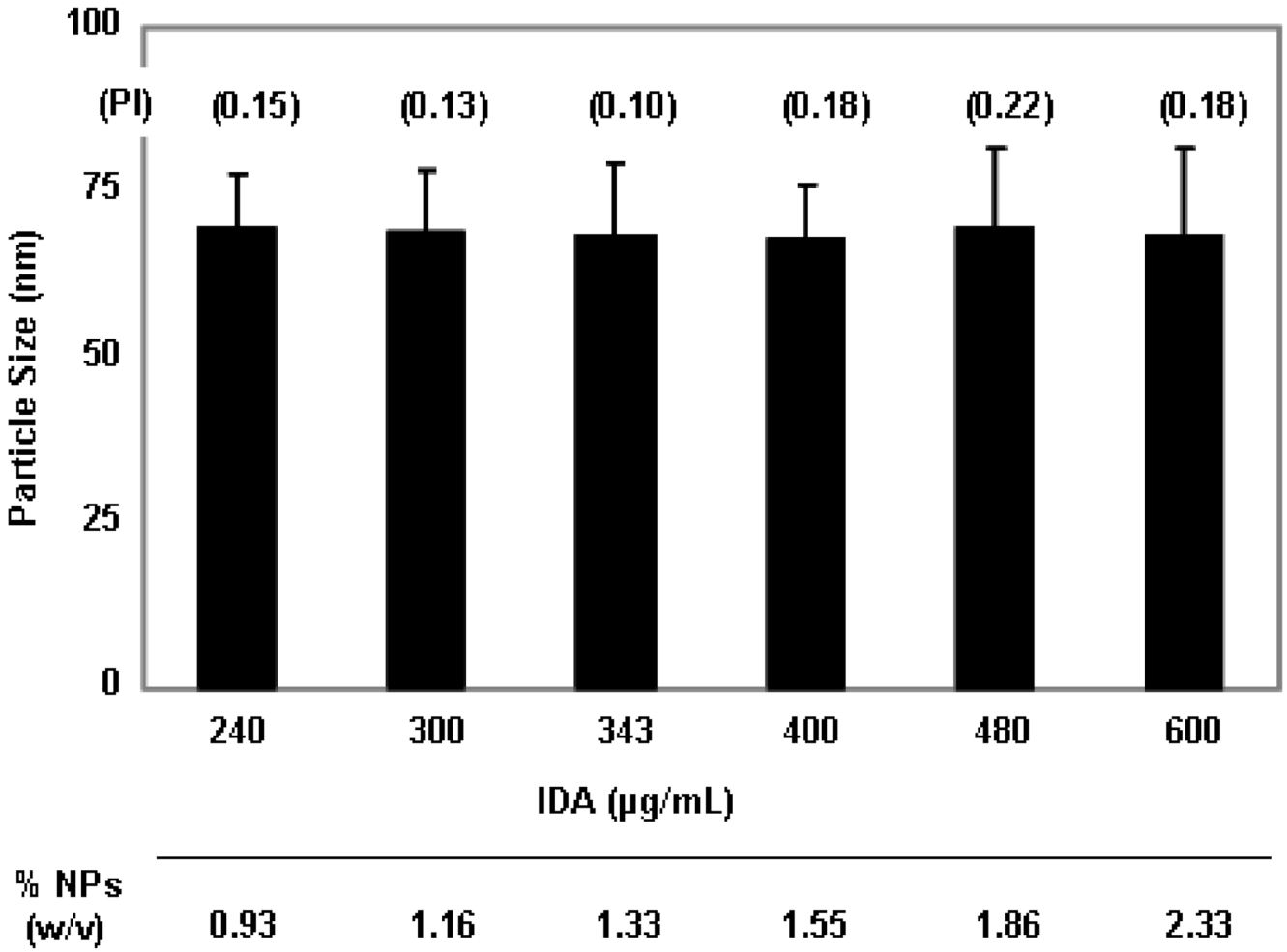

Figure 3.

Characterization of concentrated IDA-STDC NPs. IDA-STDC NPs with concentrations ranging from 240 µg up to 600 µg IDA/mL were engineered by decreasing the volume of aqueous phase in the warm o/w microemulsion while keeping the composition of oil phase (oil + surfactant + drug + ion-pairing agent) constant. Particle size, polydispersity index (PI), and the total weight of NPs (w/v) were measured. The total weight of NPs (w/v) was calculated as follows: The total weight of NPs (w/v) = [mass of the oil phase (oil + surfactant + drug + ion-pairing agent), µg] / [volume of NPs, mL]. Results of particle size measurement are expressed as mean ± SD (n = 3).

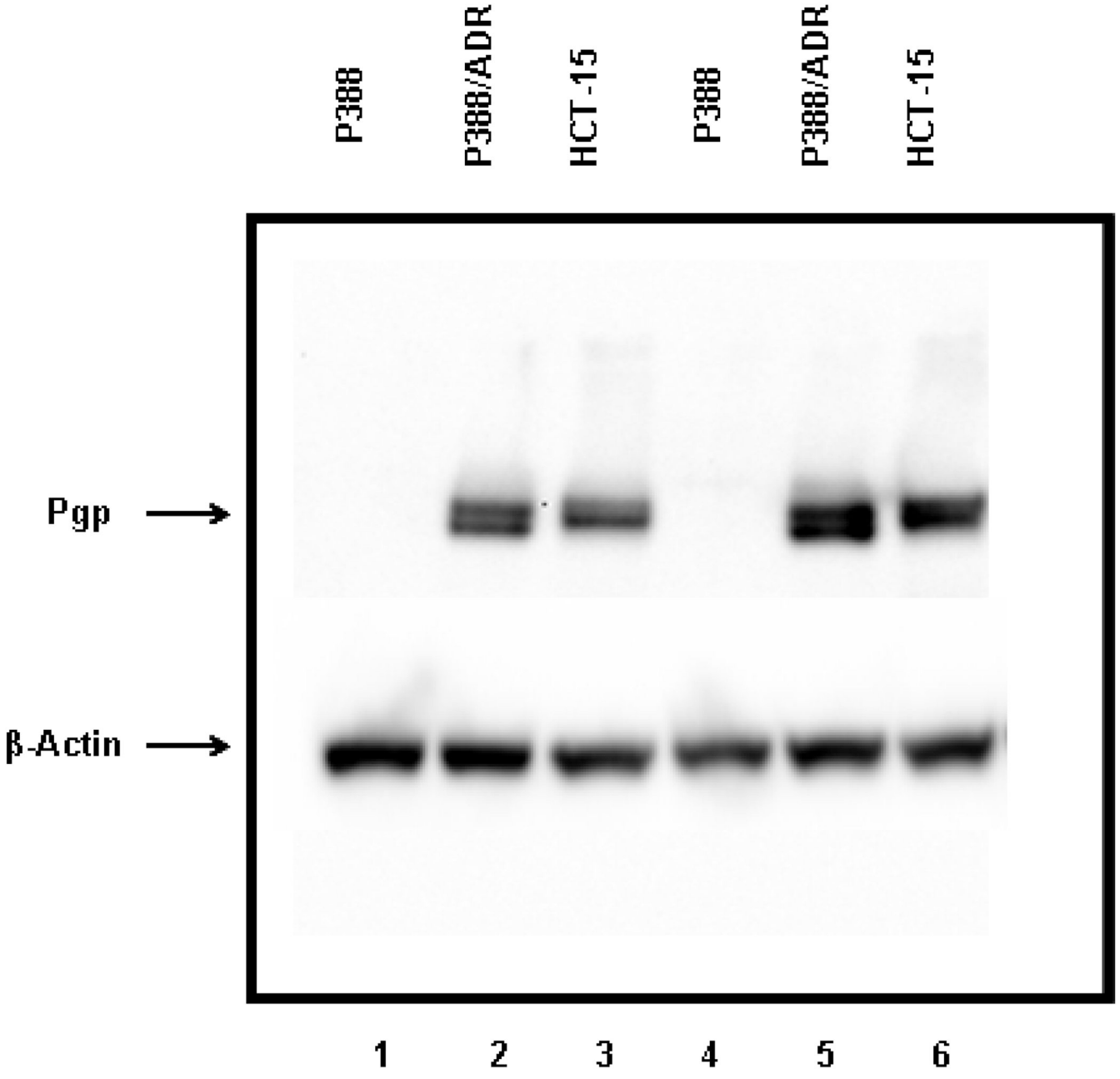

Figure 4.
Western blotting detection of Pgp in P388, P388/ADR, and HCT-15 cell lines. Forty to sixty micrograms of protein of each cell lysate was isolated using a 10% SDS/PAGE gel. Immunoblotting was performed using Mdr-1/Pgp antibody, followed by goat anti-mouse IgG-HRP. The images were then developed using enhanced chemiluminescence. β-actin was used as the loading control. Lanes 1–3: low protein load; Lanes 4–6: high protein load.

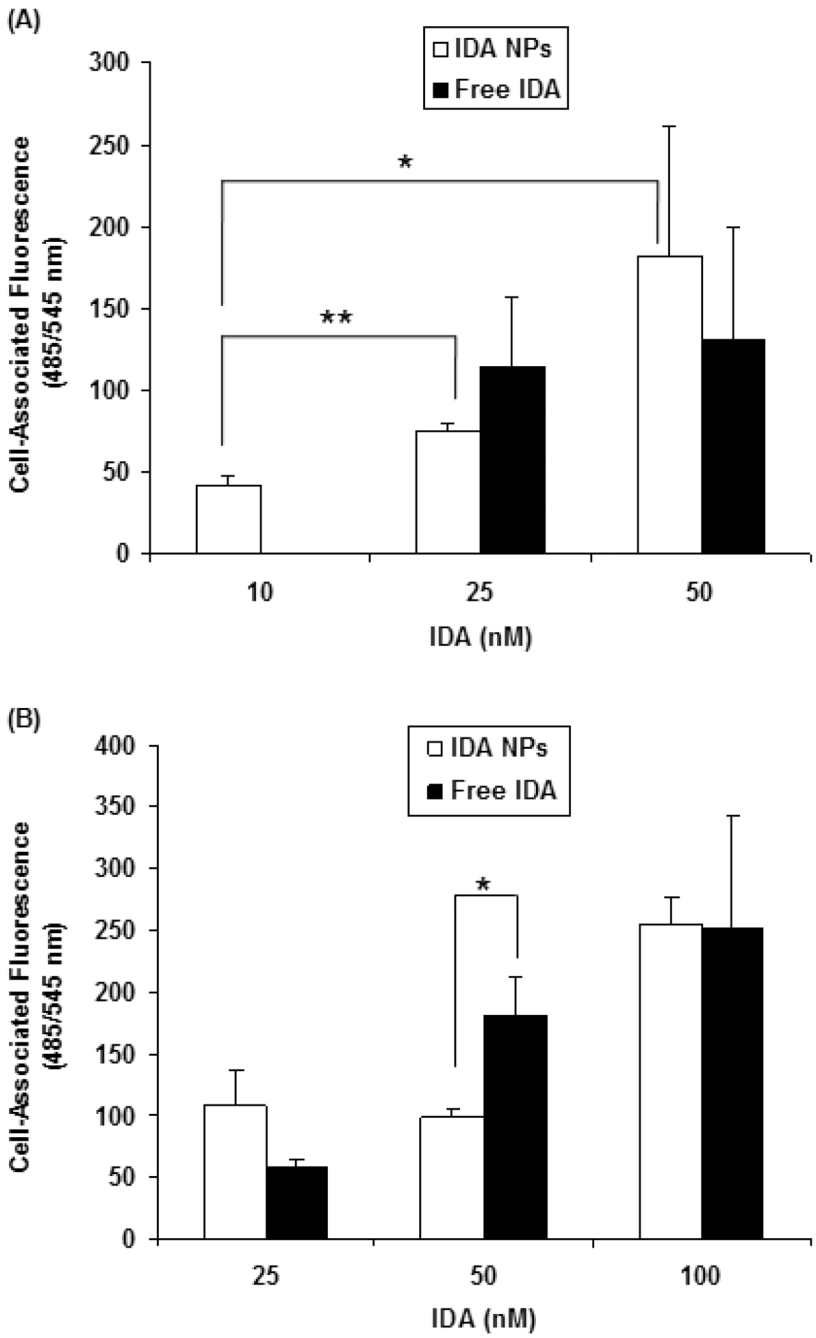

Figure 5.

Cellular uptake of free IDA and IDA NPs in (A) HL-60 and; (B) HL-60/VCR cell lines. Tested articles were added to a 12-well plate (7.5×10^5 cells/well) and incubated at 37°C for 4 hr. Cells were then transferred to 15 mL graduated tubes and centrifuged. The medium was then aspirated and replaced with fresh medium. Cell-associated fluorescence was measured at the excitation and emission wavelengths of 485 ± 20 and 545 ± 10 nm, respectively. Results are expressed as mean ± SD (n = 3). (* $p < 0.05$, ** $p < 0.01$)

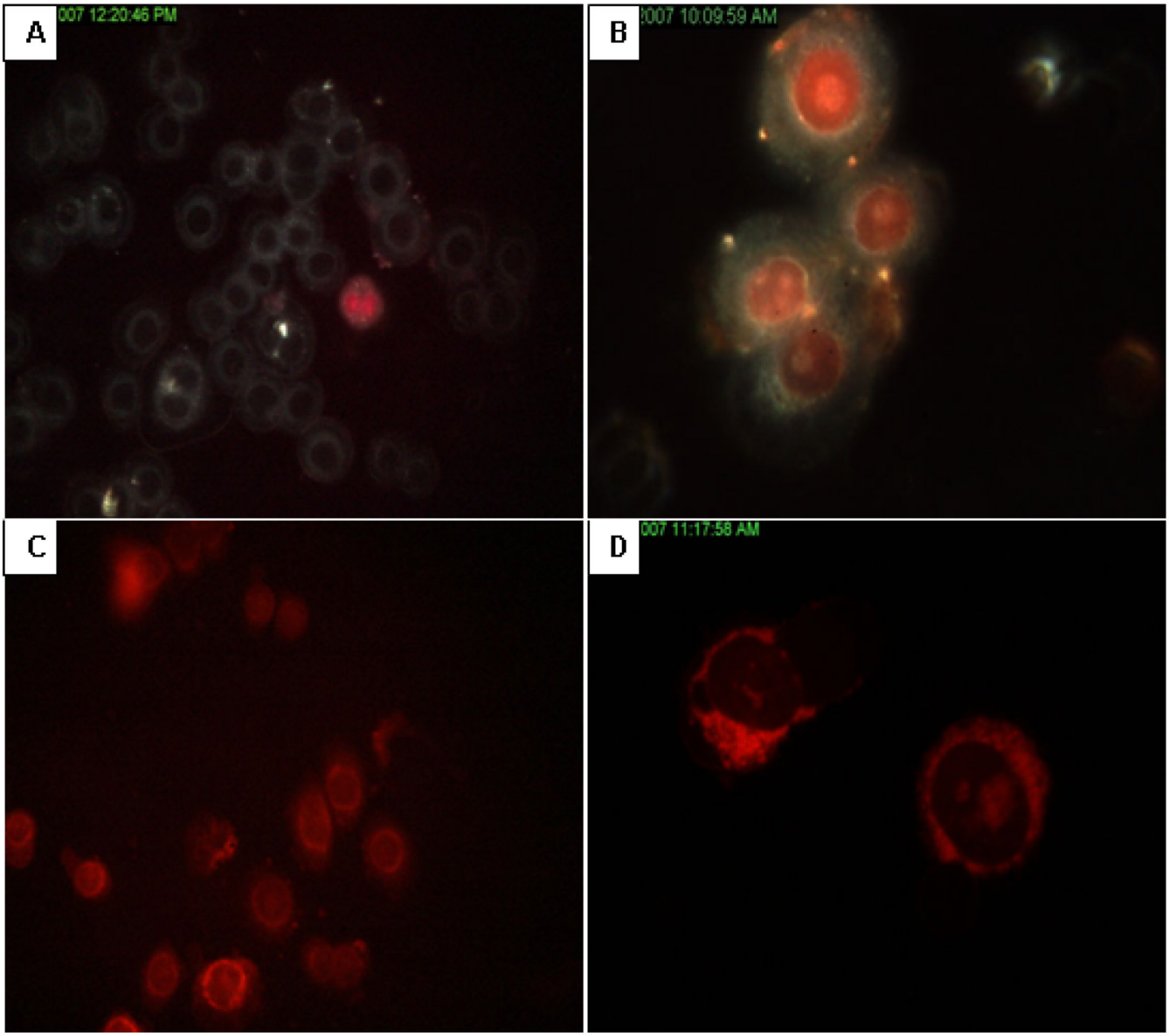

Figure 6.
Cellular uptake of free IDA or free DOX, and drug NPs in MDA-MB-468 cell line. Cells were first plated onto glass slides, and then 10 μL of tested articles were dispersed on glass slides and covered with coverslips. After 10 min, cellular uptake pictures were taken by CytoViva microscope at room temperature: (A) Free DOX; (B) DOX NPs; (C) Free IDA; (D) IDA NPs.

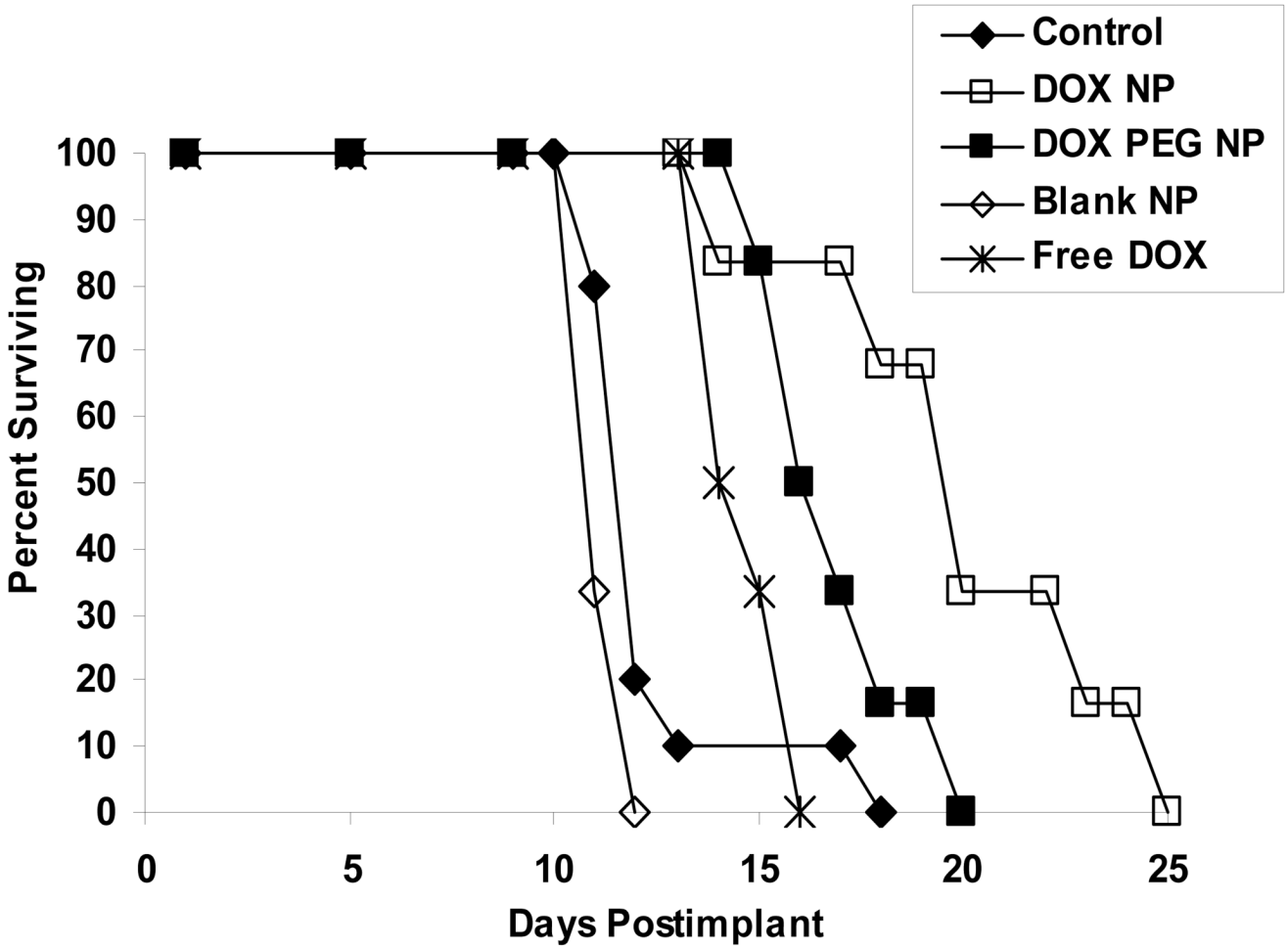

Figure 7.

Antitumor activity of free DOX and DOX NPs in mice bearing P388/ADR leukemia model. Survival curves were derived from the following different treatment groups in male CD2F1 mice inoculated i.p. with 10^5 P388/ADR cells and treated 24 hr later at the dose of 3.5 mg/kg/injection on a q4d × 3 treatment schedule: (♦) control; (□) DOX NPs; (■) DOX PEG NPs; (◊) blank NPs; (*) free DOX. The number of 25-day survivors, median day of death, and Increase in Life-Span (ILS) based on median day of death were recorded.

Table 1

Characterization of IDA and DOX NPs. Results are expressed as mean ± SD (n = 3–5)

	Particle Size* (nm)	PI	Zeta Potential (mV)	% Entrapment
IDA-STDC NPs	79.7 ± 0.2	0.112 ± 0.035	−5.7 ± 0.6	82 ± 3
IDA-STS NPs	94.7 ± 0.2	0.213 ± 0.057	−13.7 ± 2.1	85 ± 5
DOX-STS NPs	104.2 ± 1.1	0.221 ± 0.071	−14.8 ± 1.2	86 ± 6
Blank NPs	94.4 ± 0.2	0.097 ± 0.022	−10.3 ± 1.7	N/A

N/A: Not Available

*The standard deviation for each particle size is the standard deviation for the mean of three independent measurements.

Table 2

IC_{50} values (nM) of free IDA, DOX and their NP formulations in various cell lines. Results are expressed as mean ± SD (n = 4).

	HCT-15	HL-60	HL-60/ADR	HL-60/VCR	P388	P388/ADR
IDA NPs	120 ± 30	23 ± 4	240 ± 36 **	22 ± 3 **	6 ± 1	55 ± 2 *
Free IDA	129 ± 38	27 ± 4	558 ± 62 **	51 ± 6 **	4 ± 1	82 ± 4 *
DOX NPs	ND	ND	ND	ND	27 ± 4	582 ± 144 **
Free DOX	ND	ND	ND	ND	34 ± 5	5220 ± 794 **
Blank NPs †	> 1000	ND	ND	ND	> 1000	> 1000

* $p < 0.05$

** $p < 0.01$

ND: Not Determined

† The concentrations of blank NPs refer to “drug equivalent” NP concentrations